The Cambrian Kalkarindji Large Igneous Province: extent and characteristics based on new $^{40}Ar/^{39}Ar$ and geochemical data

Lena Z. Evins[a,b,*], Fred Jourdan[c], David Phillips[d]

[a] School of Earth and Geographical Sciences, University of Western Australia, 35 Stirling Highway, Crawley WA 6009, Australia

[b] Department of Mineralogy, Swedish Museum of Natural History, Box 50007, SE-10504 Stockholm, Sweden.

[c] Western Australian Argon Isotope Facility, Department of Applied Geology and JdL-CMS, Curtin University of Technology, GPO Box U1987 Perth, WA 6845, Australia. *f.jourdan@curtin.edu.au*

[d] School of Earth Sciences, The University of Melbourne, Victoria, 3010, Australia. *dphillip@unimelb.edu.au.*

* Corresponding author. Present address: Department of Mineralogy, Swedish Museum of Natural History, Box 50007, SE-10504 Stockholm, Sweden. Tel.: +46-8-51954041 Fax: +46-8-51954031

Email address: *lena.zetterstrom@nrm.se*

Abstract

The Early Cambrian Kalkarindji Continental Flood Basalt Province in northern Australia is an important Large Igneous Province (LIP) both in size and timing. Being the earliest Phanerozoic LIP it may have had a severe effect on the Early Cambrian biota. Here, we investigate the extent of this province by testing the hypothesis that the extensive Table Hill Volcanics in south-central Australia are a southern extension of the Kalkarindji province. The Table Hill Volcanics have long been considered coeval with the Antrim Plateau Volcanics and related volcanics in the Kalkarindji province; however precise age has been lacking. Here, we present new $^{40}Ar/^{39}Ar$ geochronological, and major and trace element data to investigate this possibility. One Table Hill sample yielded a plateau age of 504.6 ± 2.5 Ma (2σ), within error of recently published age data from the Kalkarindji LIP. Samples from both Table Hill Volcanics and the northern part of the province are low-Ti tholeiites with MgO-content ranging from 3 to 9 wt% and all samples are highly enriched in incompatible elements compared to primitive mantle. This, coupled with a negative Nb anomaly, suggests crustal contamination at an early stage in magma evolution or a significant contribution from the sub-continental

lithospheric mantle. Subsequent fractionation produced further elevation of the REE in the later stages of the eruptions. Subtle differences in some incompatible element ratios between the Table Hill Volcanics and northern Kalkarindji indicate some variation likely related to the assimilated crustal component or minor mantle source heterogeneity. The new geochronology data and analogous geochemical signatures confirm that the Table Hill Volcanics are a southern counterpart of the Kalkarindji province. These new data permit the areal extent of the province to be estimated at >2.1x10^6 km^2. This makes the Kalkarindji province one of the largest LIPs of the Phanerozoic. Volatile outgassing from a province of this size is likely to have had a significant impact on the climate and biosphere and may have played a dominant role in the lower-middle Cambrian mass extinction.

Keywords: Large Igneous Province, $^{40}Ar/^{39}Ar$, geochemistry, Cambrian, Australia

1. Introduction

Large igneous provinces (LIPs) represent important magmatic events in Earth history. The connection between Phanerozoic LIPs, continental rifting and mass extinctions makes them attractive targets for study (Coffin and Eldholm, 1994; Bryan and Ernst, 2008). Although LIPs are known from at least the Paleo-Proterozoic, LIPs older than the Permian have received limited attention, largely due to their poor preservation (Ernst and Buchan, 1997; Barley et al., 1997, Eldholm and Coffin, 2000). Recently, Hanley and Wingate (2000), following the earlier suggestion of Bultitude (1976), put forward that tholeiitic rocks from a vast area in northern Australia belong to a single Cambrian magmatic province. This c. 506 Ma province is named the Kalkarindji Continental Flood Basalt Province (Glass and Phillips, 2006); it is the oldest Phanerozoic LIP known. Glass and Phillips (2006) suggested that the Kalkarindji LIP coincided with the earliest major Phanerozoic mass extinction at the lower-middle Cambrian transition (see Zhuravlev and Wood, 1996; Hallam and Wignall, 1999), thereby extending the temporal correlation between LIPs and mass extinctions (see Courtillot and Renne, 2003; Hough et al., 2006) further back in time. The Cambrian subdivision is presently being revised (Babcock and Peng, 2007); in the following text we will, for

simplification, use the traditional subdivision ("Early" and "Middle") of Shergold and Cooper (2004).

Previously, the size estimates for the Kalkarindji province have ranged from >0.3x10^6 km^2 (Hanley and Wingate, 2000) to >1x10^6 km^2 (Glass and Phillips, 2006). In comparison, the areal extent of the Deccan continental flood basalt province is estimated at 1.8x10^6 km^2 (Courtillot and Renne, 2003), the Karoo province at >3x10^6 km² (e.g. Jourdan et al., 2005) and Central Atlantic Magmatic Province (CAMP) at ~10x10^6 km² (Nomade et al., 2007). The main goal with the present study is to provide an improved estimate of the size of the Kalkarindji LIP by testing the hypothesis that the extensive Table Hill Volcanics in south and central Australia are part of the same province. We also aim to provide an initial appraisal of the architecture of the Kalkarindji LIP based on petrography and geochemistry. Hereafter, we present and discuss new geochemical and high precision ^{40}Ar/^{39}Ar data in light of recently published data from different areas of the Kalkarindji LIP. We propose a revised size estimate of the Kalkarindji province, which is relevant for assessing the possible environmental effects of these eruptions and the link to the Early-Middle Cambrian mass extinction (e.g. Zhuravlev and Wood, 1996; Hough et al. 2006).

2. Geological background

Based largely on geochemical data, the Kalkarindji LIP has been shown to include the Antrim Plateau Volcanics, Helen Springs Volcanics, Nutwood Downs Volcanics, Peaker Piker Volcanics, and Colless Volcanics in northern Australia (Fig. 1). These units alone cover at least c. 300 000 km^2 (Bultitude, 1976, Hanley and Wingate, 2000). In this area the Antrim Plateau Volcanics are the most prominent with the largest outcrop area. The Antrim Plateau Volcanics also display the thickest successions with a thickness of c. 1000 m (locally 1500 m), with the volcanic successions thinning to less than 100 m in the easternmost areas

(Bultitude, 1976). The Antrim Plateau Volcanics are mainly made up of tholeiitic basalt and basaltic andesite (e.g. Bultitude, 1976) that in most areas overlie eroded Precambrian rocks; however, in some areas the Kalkarindji basalts rests on a Neoproterozoic to Early Cambrian massive reddish-brown quartz sandstone. In the Nutwood Downs area (N of Georgina basin, Northern Territory; Fig.1), the volcanics rest conformably on the Lower Cambrian Bukulara sandstone, and the lava appears to have erupted before the sandstone was lithified, as indicated by sandstone 'dykes' in the basal lava flow (Dunn, 1963; Bultitude, 1976). Some beds in the underlying sandstone may be of aeolian origin, but there are also large areas of carbonate-rich sandstone of subaqueous origin, suggesting a continental, near-shore marine or fluvial environment during the earliest volcanic activity (Sweet et al, 1974).

Early Middle Cambrian shallow-water sediments overlie the Kalkarindji volcanics. In the East Kimberleys, the Antrim Plateau Volcanics are overlain by the Middle Cambrian Headleys limestone, with the contact considered to represent a disconformity (Mory and Beere, 1988; Sweet et al, 1974; Bultitude, 1976). In the Georgina basin, the limestones overlying Helen Springs Volcanics and Peaker Piker Volcanics are in turn overlain by Middle Cambrian phosphorites (e.g. Hough et al., 2006). These deposits are related to a global sea-level rise and flooding of the North Australian craton (Freeman et al., 1990).

Sweet et al. (1974) and Mory and Beere (1988) have described four members in the Antrim Plateau Volcanics, from oldest to youngest: The Malley Spring member, a c. 5 m thick sandstone; the Mt Close Chert member, a c. 5 m thick stromatolitic chert; the Bingy Bingy basalt member, a c. 40 m thick glomeroporphyritic basalt with locally developed columnar jointing; the Blackfella Rockhole member, a c. 70 m thick unit, comprising volcanic breccia and minor basaltic lavas. These members are placed within much thicker sections of the generally fine to medium grained basaltic rocks which make up the majority of the volcanic pile. The Bingy Bingy basalt and the Blackfella Rockhole members are both found

in a c. 10 500 km^2 area straddling the Western Australia – Northern Territory border. Large scale cross-bedding in the Malley Spring member indicates an aeolian depositional environment, suggesting that this member may be related to the sandstone locally underlying the Antrim Plateau Volcanics (Mory and Beere, 1988). There are a number of areas where layers of intercalated sediments and pyroclastics have been found; these are best described by Sweet et al. (1974). Most of these interbeds are thin and of limited extent and occur at different stratigraphic horizons. The intercalated sandstone and siltstone were deposited under subaqueous conditions (Sweet et al., 1974). In the Antrim Plateau Volcanics, the Mount Close Chert Member, about halfway up the succession, indicates a hiatus in volcanic activity (Mory and Beere, 1988). A number of chert beds have also been described by Sweet et al. (1974, and references therein). The Blackfella Rockhole member in the upper part of the succession also contains some thin lenses of sandstone and siltstone.

Bultitude (1976) first suggested that the Paleozoic Table Hill Volcanics in the Officer basin, Western Australia, may be related to the Antrim Plateau Volcanics several hundred km's away. (Fig. 1), . This correlation has since been reiterated in several studies (Jackson & van der Graaf, 1981; Townson, 1985; Walter et al. 1995; Hanley and Wingate, 2000; Glass and Phillips, 2006); however, attempts to date the Table Hill Volcanics by Rb-Sr on pyroxene and whole rock yielded a c. 560 Ma age (Compston, 1974; Veevers, 2004) and K-Ar whole rock dating yielded a c. 480 Ma age (Stevens and Apak, 1999). This discrepancy and lack of a reliable age of the Table Hill Volcanics has barred a definitive conclusion regarding the Table Hill-Kalkarindji connection. Thus, the Table Hill-Kalkarindji connection has been based on geochemical (Gole, 2001; Glass and Phillips, 2006) and stratigraphic relationships (e.g. Grey et al., 2005).

The Table Hill Volcanics were first described by Peers (1969) and are named after the main outcrop in the c. 525 000 km^2 Officer basin (Grey et al., 2005; Jackson and van

Der Graaf, 1981). The Table Hill Volcanics are synonymous with the Kulyong Volcanics in South Australia, as indicated by field and aeromagnetic evidence (Townson 1985). The Table Hill Volcanics are found in an area of c. 182 000 km^2, including intrusions located in the Savory Sub basin (NW Officer basin; Townson, 1985). There are also reports of possibly related mafic intrusions in the Canning basin, north of the Savory sub basin (D. Maidment, pers. comm., Fig1.). Many mafic sills and dykes in the sedimentary rocks of the Officer basin are probably feeders to the Table Hill Volcanics. Two sills have been dated: i) U-Th-Pb SHRIMP analyses of zircons yielded a weighted mean $^{207}Pb/^{206}Pb$ age of 508±5 Ma (95% confidence level[1], MSWD=0.2, P=1.0; Macdonald et al., 2005); ii) nanoSIMS Pb-Pb dating of zirconolite yielded a weighted mean $^{207}Pb/^{206}Pb$ age of 504±18 Ma (95% conf. MSWD=0.93, P=0.49, Stern et al., 2005).

The Table Hill Volcanics are 26 m thick in the type section (Table Hill, 26°28'S,126°53' E), with a maximum reported thickness of 118 m (Yowalga 2 drill core; Townson, 1985). In the Yowalga 2 drill core, as well as in outcrop, two thick flows are separated by a sandy weathered interval. Additional, thinner lava flows are also present (Townson, 1985). In the Empress 1 and 1A drill cores the Table Hill Volcanics attain a thickness of 84 m with 6 flows defined by wireline density core logging (Stevens and Apak, 1999). Stratigraphically, the Table Hill Volcanics are younger than the Marinoan (610-560 Ma) Lungkarta Formation and older than the Devonian Wanna Formation (Grey et al., 2005). At Table Hill, and other major outcrop areas, the volcanics are overlain by the Devonian-Carboniferous Lennis sandstone (Townson, 1985); elsewhere, the Table Hill Volcanics are overlain by the Permian Paterson formation (Jackson and van Der Graaf, 1981).

3. Sample descriptions

[1] All ages in this study are reported at 95% confidence level, otherwise indicated

156 The samples investigated in this study come from different areas of the Antrim Plateau
157 Volcanics and from drill cores intersecting the Table Hill Volcanics (Empress 1 and Empress
158 1A drill cores, GSWA; Table 1).

159 The 12 Antrim Plateau Volcanics samples studied here were collected during a
160 field trip to the East Kimberleys, northern Australia in July 2005, in order to sample rocks
161 representative of different stages of the eruptive sequence. Samples 084, 085, 086A, 087 and
162 091 originate from an area where chromite has been recovered from basaltic whole rock
163 samples and from detrital river sand (Reddicliffe, 1980). These samples comprise fine- to
164 medium grained basalt with low levels of alteration (except 086A) and are considered an early
165 eruptive phase of the Kalkarindji LIP. Sample 086A is a severely altered rock, intensely green
166 from chloritisation. Sample 022, a fine grained basalt, is collected from one of the first flows
167 in the volcanic succession in the Purnululu area, close to the contact to the underlying
168 sandstone. These samples are grouped together as "Early Antrim Plateau Volcanics".

169 Sample 097 is a weakly porphyritic basalt, sampled c. 2 km NW of the
170 "chromite area". Samples 020 and S2-33, both with visible magnetite grains in hand
171 specimen, are from locations in the middle part of the succession near Purnululu. Sample 027
172 was collected from a well-exposed area of massive basalt c. 70 km south of the Purnululu area
173 (Marella Gorge); thin section studies reveal a slightly trachytic texture and feldspar
174 microphenocrysts, some with minor alteration. Samples D04 and 039 are from the Bingy
175 Bingy basalt member, and represent the upper part of the succession; Sample D04, which is
176 distinctly red-brown in colour due to alteration, exhibits a spotted appearance in hand sample
177 from altered plagioclase glomerocrysts. The glomerocrysts are less visible in sample 039,
178 which is a darker rock with weakly developed columnar jointing. In both samples the
179 plagioclase glomerocrysts are severely altered. These samples represent the main and late

180 phases of the eruptions, respectively and are grouped together as “Main-Late Antrim Plateau
181 Volcanics”.
182 The Empress drill cores in the Officer basin (Fig. 1) were described by Stevens
183 and Apak (1999) and intersect 84 m of Table Hill Volcanics. As interpreted from the sonic
184 and density wireline logs, the intersected section of Table Hill Volcanics comprises 6 flows
185 (Stevens and Apak, 1999). For this study, we sampled all but the lowermost flow. The
186 samples from the lower part of the succession (flows 2 and 3) are amygdaloidal and more
187 altered than samples from the upper part (flows 5 and 6). The samples comprise fine- to
188 medium grained basalts containing plagioclase, clinopyroxene and opaques. Very fine grained
189 secondary alteration minerals, occur mainly in the fine grained matrix but also to some degree
190 in plagioclase microphenocrysts. Some are weakly porphyritic with plagioclase laths up to 1
191 mm, although plagioclase rarely forms crystals larger than c. 300 μm.
192
193 **4. Methods**
194 In preparation for geochemical analyses, weathered edges were removed from the samples,
195 which were then crushed and milled using a tungsten carbide ring mill. Major elements of all
196 samples were analysed by X-ray Fluorescence (XRF) at the Advanced Analytical Centre
197 (AAC) at James Cook University, Townsville (Australia) using a Bruker-AXS S4 Pioneer X-
198 ray Fluorescence Spectrometer. The analytical errors on the major elements range from 0.3 -
199 1.8% (1σ). The Table Hill samples were analysed for trace elements by full acid digestion
200 ICP-MS (Varian ICP-MS 820) at the AAC, Townsville with analytical errors ranging from 2
201 to 7 % (1σ). These samples were analysed as two batches (EMP1 and EMP1A). For the
202 second batch (EMP1A samples), elevated Ti values from ICP-MS likely resulted from
203 contamination, prompting the use of XRF data for the Ti content for these samples. In
204 addition, the second batch of ICP-MS analyses had an unreasonably high Pb blank and thus,

205 Pb values from the second batch values are not corrected for blank. The Antrim Plateau
206 samples were analysed for trace elements by full acid digestion ICP-MS (Cr, V by ICP-AES)
207 at SGS in Perth (Australia).

208 Five of the least altered samples from drill cores Empress 1 and 1A were
209 selected for $^{40}Ar/^{39}Ar$ dating. Optically transparent plagioclase feldspar grains (100-200 μm-
210 size) were separated from four samples (EMP1 212, EMP1 253, EMP1 255, EMP1A 238). An
211 additional sample (EMP1 214), with very fine grained plagioclase, was analysed as whole
212 rock only. Plagioclase was separated using a Frantz magnetic separator, and then carefully
213 hand-picked under a binocular microscope. After initial $^{40}Ar/^{39}Ar$ results were obtained from
214 these samples, two additional plagioclase separates (from EMP1 255 and EMP1A 238),
215 comprising transparent grains free of cracks and cloudy regions (potential reservoirs for
216 sericite), were leached for 1 minute in diluted HF (2N) and then thoroughly rinsed with
217 distilled water in an ultrasonic cleaner.

218 The $^{40}Ar/^{39}Ar$ isotope analyses were performed at the Noble Gas Geochronology
219 and Geochemistry laboratory, the University of Melbourne and at the Western Australian
220 Argon Isotope Facility (WAAIF; Curtin University and the University of Western Australia).
221 The analytical procedures at the two different laboratories are described separately in the
222 following text.

223 $^{40}Ar/^{39}Ar$ analytical procedures for analyses conducted at the University of
224 Melbourne laboratory were analogous to those described by Phillips et al. (2007). Step-
225 heating analyses of plagioclase and whole rock samples were carried out using a tantalum
226 furnace connected to a VG3600 mass spectrometer equipped with a Daly detector. The
227 neutron fluence monitor used was GA1550 biotite (98.8 ± 0.5 Ma; Renne et al., 1998), which
228 yielded J-values ranging from 0.013046 ± 0.000032 (0.24%) to 0.013062 ± 0.000023
229 (0.17%). Mass discrimination (mean = 1.0075 ± 0.16% per atomic mass unit) was monitored

by measuring air aliquots from a Doerflinger pipette. Correction factors for interfering isotopes were $(^{39}Ar/^{37}Ar)_{Ca}$ = 6.79 x 10^{-4} (± 0.7%), $(^{36}Ar/^{37}Ar)_{Ca}$ = 2.70 x 10^{-4} (± 1.7%) and $(^{40}Ar/^{39}Ar)_{K}$ = 5.0 x 10^{-4} (± 39%).

$^{40}Ar/^{39}Ar$ analyses conducted at WAAIF employed step heating on a MAP215-50 mass spectrometer. The samples were step-heated using a 110 W Spectron Laser Systems, with a continuous Nd-YAG (IR; 1064 nm) laser rastered over the sample packed in 0-blank Nb foil, during 1mn to ensure an homogenously distributed temperature. Fish Canyon sanidine (FCs) was used as the fluence monitor (28.030 ± 0.053 Ma; Jourdan and Renne, 2007), giving J-values ranging from 0.008794±0.000027 (0.31%) to 0.008738±0.000013 (0.15%), determined as the average and standard deviation of J-values of the small wells for each irradiation disc. Mass discrimination at WAAIF, mass discrimination was monitored using an automated air pipette and provided a mean value of 1.004628 ± 0.21% (1σ) per atomic mass unit (a.m.u.). Correction factors for interfering isotopes were $(^{39}Ar/^{37}Ar)_{Ca}$ = 7.30x10^{-4} (± 11%), $(^{36}Ar/^{37}Ar)_{Ca}$ = 2.82x10^{-4} (± 1%) and $(^{40}Ar/^{39}Ar)_{K}$ = 6.76x10^{-4} (± 10%).

Criteria for the determination of age plateaus are as follows: plateaus must include at least 70% of ^{39}Ar. The plateau should be distributed over a minimum of 3 consecutive steps, coincident at the 95% confidence level and with a probability of fit (P) of at least 0.05. Plateau ages are given at the 2σ level and are calculated using the mean of all the plateau steps, each weighted by the inverse variance of their individual analytical error. Mini-plateaus are defined similarly except that they include between 50% and 70% of ^{39}Ar.

Calculated uncertainties in integrated and plateau ages include errors in the $^{40}Ar^*/^{39}Ar$ ratios of the monitors, but exclude errors associated with the age of the monitor and the decay constant (internal errors only, see discussion by Min et al., 2000).

5. Results

255 5.1. Major and trace element geochemistry

256 Thin section investigations combined with major element and trace element data
257 (Supplementary data Tables 1 and 2) show that the petrography and chemistry of the studied
258 samples agree with published data from the Kalkarindji LIP and that the chemistry of the
259 Table Hill Volcanics closely resembles that of the Antrim Plateau Volcanics (Bultitude, 1976;
260 Hanley and Wingate, 2000; Gole 2001; Glass, 2002; Gole and Thornett, 2003; Glass and
261 Phillips, 2006). The samples analysed here are tholeiitic basalts and basaltic andesites based
262 on the Cox et al (1979) classification, with relatively low TiO_2 (0.7 to 1.4 wt%) and MgO
263 levels of 4.3 to 8.5 wt%. This corroborates previously reported MgO values of c. 3 to 9 wt%
264 (Bultitude, 1976; Glass, 2002). SiO_2, TiO_2, ,Fe_2O_3, P_2O_5, and to a certain degree K_2O show a
265 negative co-variation with MgO (Fig. 2). There is a positive co-variation of Al_2O_3 and CaO
266 with MgO; however Na_2O shows no correlation with MgO, likely due to alteration effects.
267 The major element data can be divided in three groups: 1) MgO 7.5 – 9 wt%, TiO_2 <0.85 wt%
268 (Early); 2) MgO 6.5 - 7.5 wt%, TiO_2 0.7 - 1.1 wt% (Main); and 3) MgO 3.8 - 5.8 wt%, TiO_2 1
269 - 2 wt% (Late). Only one of the Main-Late Antrim Plateau samples (020) plots in the Main
270 group. The Milliwindi dolerite, a major feeder dyke in the Kimberleys, Western Australia
271 (Fig. 1, Hanley and Wingate, 2000) also plots in the Main group (Fig 2). The Empress (Table
272 Hill) samples plot in both the Early and Main groups (Fig. 2), although the majority of the
273 data is associated with the Main group. Both samples from the Bingy Bingy basalt (D04 and
274 039), as well as samples 027 and 091, plot in the Late (low MgO) group in Fig. 2.

275 The trace elements of all samples, normalised to primitive mantle (Sun &
276 McDonough 1989), display almost identical patterns on a spider diagram (Fig. 3). The Main -
277 Late Antrim Plateau Volcanics have elevated trace element concentrations compared to those
278 from the Early Antrim Plateau Volcanics. One heavily altered sample (086A) from the Early
279 Antrim Plateau Volcanics was analysed with the aim of identifying the elements most mobile

280 during alteration; these elements are Cs, Rb, Ba, K, Sr and possibly Pb (Fig 3). A pronounced
281 negative Nb-anomaly coupled with positive K and Pb anomalies define the characteristic
282 shape of this trace element pattern. All samples from the Empress drill core show slightly
283 elevated Zr compared to Antrim Plateau Volcanics. The most incompatible elements are
284 strongly enriched which is exemplified by Rb/Y_n (primitive mantle, Sun & McDonough,
285 1989) ratios ranging from 6 to 40 (excluding 086A). The chondrite-normalised REE pattern
286 shows general enrichment of REE and significant enrichment of the LREE/HREE (Fig. 4).
287 The Early Antrim Plateau Volcanics are easily distinguished from the rest of the
288 samples by elevated Cr content (c. 300 ppm), compared with Main - Late Antrim Plateau
289 Volcanics and Table Hill Volcanics (Fig. 5). All Table Hill Volcanics samples contain
290 between 60 and 140 ppm Cr (Fig. 5) and they show most chemical similarity to the Main
291 Antrim Plateau Volcanics rocks. The trace element data plot in three groups on several
292 variation diagrams (Fig. 5); these groupings correlate well with the Early, Main and Late
293 Antrim Plateau Volcanics. In several of these diagrams the Table Hill Volcanics show
294 somewhat elevated trace element values for a given Ti value; this is most pronounced for Zr,
295 but Y, Nd and La show similar trends (Fig. 5). This minor elevation of Y, Zr and LREE
296 appears to be a distinguishing feature of the Table Hill Volcanics compared to the rest of the
297 Kalkarindji province (except altered sample 086A, possibly indicative of La mobility during
298 extreme alteration). The Y and LREE enrichment of the Table Hill Volcanics, compared to
299 the Antrim Plateau Volcanics, results in lower, more variable Ti/Y ratios for the Table Hill
300 Volcanics (Fig. 5). On a Ce/Yb vs. TiO_2 diagram (Fig 4.), two Table Hill samples have,
301 together with TH003 (Glass and Phillips, 2006), higher Ce/Yb ratios for a given Ti value.
302 Altered sample 086A also has an anomalously high Ce/Yb; there is, however, no general
303 correlation between LOI (loss-on-ignition, as a measure of alteration) and Ce/Yb. Ce/Yb_n

304 (normalised to primitive mantle, Sun & McDonough, 1989) ranges from 2.7 to 4.2 (086A
305 excluded).
306
307 5.1. $^{40}Ar/^{39}Ar$ geochronology
308 $^{40}Ar/^{39}Ar$ age dating was conducted on five Table Hill samples at University of Melbourne,
309 with two of these samples also analysed at Curtin University. The full $^{40}Ar/^{39}Ar$ data set is
310 reported in Supplementary data, Table 3. All five samples have total fusion ages between 480
311 and 590 Ma (Table 2). However, despite efforts to handpick unaltered plagioclase grains from
312 three samples, none of the initial five analyses yielded concordant results, indicating a
313 combination of Ar loss and alteration, ^{39}Ar recoil, and excess argon contamination (Fig. 6). In
314 an attempt to improve on these results, rigorous sample treatment (e.g. HF leaching) was
315 applied to samples EMP1 255 and EMP1A 238. This resulted in one mini-plateau age of
316 504.6±2.5 Ma (2σ; MSWD = 1.6; P = 0.09; Fig. 6) for sample EMP1 255, whereas sample
317 EMP1A 238 still failed to yield concordant data. The Ca/K spectra of sample EMP1 255
318 show a tilde-shaped pattern not observed on the age spectrum. This might reflect: i) the
319 presence of a small amounts of sericite with a syn-eruptive age (Jourdan et al., submitted); ii)
320 plagioclase compositional zoning or; iii) cryptic antiperthite exsolution combined with ^{39}Ar
321 and ^{37}Ar recoil effects (e.g., De Min et al., 2003). The absence of any co-variation between
322 the ages and Ca/K ratios suggests that whatever caused the variation in Ca/K ratios did not
323 have a significant effect on the age of this sample. In the inverse isochron diagram (not
324 shown), all samples yielded poorly defined initial $^{40}Ar/^{36}Ar$ values (Table 2), due to a strong
325 clustering of the data near the $^{39}Ar/^{40}Ar$ axis. This prevents the determination of statistically
326 meaningful isochron ages and $^{40}Ar/^{36}Ar$ intercepts for these samples.
327
328 **6. Discussion**

329 6.1 Age of the Kalkarindji province

330 The results from combined geochemistry and geochronology confirm previous suggestions
331 that the Table Hill Volcanics should be considered a part of the c. ~506 Ma Kalkarindji LIP.
332 Although four of the five samples analysed failed to produce meaningful results, a plagioclase
333 separate of sample EMP1 255 yielded a statistically robust mini-plateau (66% ^{39}Ar released)
334 ^{40}Ar/^{39}Ar age at 504.6 ± 2.5 Ma (Fig 6). Here we compare this new age with existing
335 geochronology data in order to establish the current state of knowledge regarding the timing
336 of Kalkarindji volcanism. Efforts to date the Table Hill Volcanics started a few decades ago,
337 with a single pyroxene-whole rock Rb-Sr analysis, which yielded an isochron age of 564 ± 40
338 Ma (Compston, 1974; recalculated by Veevers, 2004). The large error associated with this
339 Rb-Sr age renders it of limited applicability. Stevens and Apak (1999) obtained a K-Ar whole
340 rock age of 484 ± 8 Ma (2σ) on one sample (Empress 1A, 215.9-216.5) of the Table Hill
341 Volcanics. However, K-Ar ages obtained from old, and particularly altered, rocks are of
342 uncertain reliability, due to difficulties in verifying the age data using internal criteria, as is
343 possible with ^{40}Ar/^{39}Ar age spectra or U/Pb concordia. Hanley and Wingate (2000) and
344 MacDonald et al. (2005) obtained U-Pb SHRIMP ages of 513 ± 12 (2σ) and 508 ± 5 Ma (2σ),
345 respectively, from the Milliwindi and Boondawari dolerites (Fig. 1). However, high-
346 resolution geochronology requires very precise data, which is normally only achievable with
347 the ^{40}Ar/^{39}Ar dating method or with the U-Pb dating of zircon using thermal ionisation mass
348 spectrometry (TIMS). For the Kalkarindji LIP, two statistically reliable ^{40}Ar/^{39}Ar ages of
349 507.5 ± 1.6 Ma (Helen Springs; MSWD = 0.89; P = 0.55) and 504.7 ± 2.2 Ma (Antrim
350 Plateau; MSWD = 0.89; P=0.09) were obtained by Glass and Philips (2006). Therefore,
351 including the age obtained in this study, the total number of precise and reliable ages for the
352 Kalkarindji province sum to three. It is worth noting that two of the three ages have been
353 derived from mini-plateau (52% and 66% of ^{39}Ar released, respectively) age spectra,

354 indicating that a significant part of each age spectra is perturbed. For major LIPs such as
355 CAMP or the Karoo, there are currently ~60 (e.g. Nomade et al., 2007) and ~80 (e.g. Jourdan
356 et al., 2008) plateau and mini-plateau ages available, respectively; statistically filtered
357 amongst a larger dataset. This significant number of analyses has been shown to be the
358 minimum required to understand the geodynamic history of a LIP. The present data suggest
359 that the Kalkarindji LIP was emplaced around ~506 Ma; however more precise age
360 estimation, determination of magmatic duration and any evaluation of magmatic migration,
361 temporal chemical evolution, and synchronicity with environmental events, require a much
362 larger dataset. This undoubtedly warrants a significant dating program on the Kalkarindji
363 province (in progress).
364
365 6.2 Geochemical characteristics of the Kalkarindji province
366 All current samples from the Table Hill Volcanics and the Antrim Plateau Volcanics exhibit
367 the same enrichment in highly incompatible elements such as U, Th and LREE. Coupled with
368 a prominent negative Nb anomaly, this indicates either crustal contamination or a contribution
369 from the sub-continental lithospheric mantle. The REE pattern confirms a slight enrichment
370 of the mantle source of the Table Hill Volcanics. The absence of significant MREE/HREE
371 fractionation (e.g. Gd/Yb_n = 1.3-1.5) indicates the absence of garnet in the magma source
372 region and thus constrains the depth of melting to a shallow spinel-bearing source (<25-30 kb,
373 corresponding to a maximum depth of 80-100 km; e.g. Robinson and Wood, 1998).
374 Unpublished $^{87}Sr/^{86}Sr_i$, $^{143}Nd/^{144}Nd$ and $\delta^{18}O$ isotopic data (Glass, 2002) obtained on samples
375 from the northern part of the Kalkarindji LIP suggest early crustal contamination of the
376 magma source with later fractionation (Glass et al., 2006). A similar crustal contamination
377 signature is also evident in the current trace element data, at least for the early, least
378 fractionated samples of the Table Hill Volcanics.

379 The most primitive composition is shown by sample 022 with 8.5 wt% MgO;
380 this basalt was sampled from one of the earliest flows in the Purnululu area. It is chemically
381 very similar to other Mg-rich basalts of the Antrim Plateau Volcanics, indicating that an MgO
382 content of 7 - 9 wt% is characteristic of early Antrim Plateau Volcanics flows. These rocks
383 also exhibit the lowest Ti and incompatible element concentrations, as would be expected for
384 the least fractionated rocks of a series. Another distinctive feature of the early Antrim Plateau
385 Volcanics is the elevated Cr_2O_3 contents. This particular feature is not shared by the earliest
386 (2^{nd} flow), most Mg-rich Table Hill basalt studied here, despite a similar MgO content. The
387 elevated Cr_2O_3 content is partly explained by the presence of Cr-rich pyroxene xenocrysts in
388 these rocks (Glass, 2002). All early Antrim Plateau Volcanics samples (excluding 022) in the
389 current study originate from the "chromite area" SE of Spring Creek, WA, where chromite
390 occurs both in outcrop and river sand (Reddicliffe, 1980). Although no chromite was
391 observed in thin section, it is possible that the elevated Cr_2O_3 values are related to rare
392 chromite grains in these rocks. Alternatively, unusual magma chamber conditions may have
393 limited the crystallization of chromite and/or Cr-rich pyroxene during early differentiation
394 processes, thereby enriching the magma in Cr_2O_3.
395 The main and late stages of the Kalkarindji eruptions produced more
396 fractionated rocks. Our study shows that the lava flows at Marella Gorge (Purnululu area,
397 WA) are chemically identical to the Bingy Bingy basalt member and represent one of the later
398 stages of the eruptive sequence. The Bingy Bingy basalt member comprises a large flow field
399 covering c. 10 500 km^2 with an average thickness of c. 40 m (Sweet et al., 1974; Mory and
400 Beere, 1988), yielding an approximate eruptive volume of c. 400 km^3. The characteristic
401 glomeroporphyritic texture suggests that the erupted lava was partially crystallised before
402 eruption. The textural difference between the chemically identical Bingy Bingy and Marella
403 Gorge basalts indicates that the process causing partial crystallisation did not change bulk

chemistry. Therefore, the trigger for partial crystallisation may be related to magma chamber dynamics and degassing behaviour.

6.3 Chemical similarity between Antrim Plateau Volcanics and Table Hill Volcanics

In order to evaluate the chemical similarity between the Table Hill Volcanics and Antrim Plateau Volcanics, selected incompatible element ratios (normalised to primitive mantle; Sun & McDonough, 1989) are listed in Table 5, and compared with published data from the central Deccan province as an example of a typical continental flood basalt (Melluso et al., 2004). For the current samples, Ce/Yb_n ratios do not vary significantly between the Antrim Plateau Volcanics and Table Hill Volcanics. The more fractionated rocks have somewhat higher Ce/Yb_n ratios (c. 4), but the average values are slightly lower than those of the Central Deccan: (~3.5; Table 3; Melluso et al., 2004). This pattern is also observed for Ce/U_n ratios, although there is some variation in the U contents of the early Antrim Plateau samples, which results in elevated average Ce/U_n values for the Antrim Plateau Volcanics. The ratios most pertinent to the comparison are P/Nd_n and Ti/Y_n. Both element pairs have almost identical bulk partition coefficients; therefore the ratios should be invariant if the source is homogenous and no crustal contamination is present. It is apparent from Fig. 7 (see also Table 3) that the Antrim Plateau Volcanics and Table Hill Volcanics have analogous compositions and are distinct from the Deccan samples. Also, the Kalkarindji LIP is relatively depleted in HFSE, as illustrated by low P/Nd_n ratios. These characteristics were also observed by Glass and Phillips (2006).

The Deccan basalts include both low TiO_2 (1.2 - 1.5 wt%) and high TiO_2 (1.6 - 3.2 wt%) rocks, whereas the Kalkarindji samples are all low TiO_2 rocks (maximum of 1.4 wt%). This produces a significantly lower Ti/Y_n for the Kalkarindji. In addition, some intra-province variation exists, as Ti/Y_n differs between the Antrim Plateau Volcanics and Table

Hill Volcanics. However, the overall geochemical similarity between the Table Hill Volcanics and Antrim Plateau Volcanics suggests a common parental magma. The observed subtle differences in degree of LREE enrichment and incompatible element ratios are likely be due to differing composition in crustal contamination during two or more stages of magma evolution.

The elemental composition of the Antrim Plateau Volcanics indicates that the least fractionated basalts occur at the base of the succession, with the more fractionated rocks present in the middle and upper levels of the succession. For the Table Hill Volcanics, no such pattern was observed. The uppermost sample in the Empress drill core (flow 6) has a more Mg-rich composition than flows 4 and 5. Flow 4 (samples EMP1255 and EMP1253) appears to be the most fractionated with the lowest MgO, and highest Zr, U and Pb contents (these elements are also elevated in flow 2). This may be due to the addition of somewhat more primitive, less contaminated magma after the eruption of flow 4. These differences are quite subtle (all Table Hill samples would fall in the "Main" group of Kalkarindji lavas) and the local flow stratigraphy is only apparent due to drill core sampling. It is likely that similar subtle differences are present in the Antrim Plateau Volcanics succession, but this requires a more detailed study of the flow stratigraphy. The overall stratigraphic characteristics of the Antrim Plateau Volcanics are not encountered in the Empress drill core: the later stages with glomeroporphyritic basaltic andesite and volcanic breccia appear to be lacking. However, the erosional upper contact of the Table Hill Volcanics in the Empress drill core suggests that the later stages of the Table Hill Volcanics were eroded before deposition of the overlying sediments.

6.4 Extent of the Kalkarindji province

453 The data presented here demonstrates unambiguously that the Table Hill Volcanics should be
454 included in the Kalkarindji LIP. Therefore we propose that the extent of the Kalkarindji is at
455 least $2.1x10^6$ km^2, thus making it one of the largest Phanerozoic LIPs. However, the problem
456 of the extent of the Kalkarindji LIP is far from solved, since there are many other areas that
457 may be part of the province (see Glass and Phillips, 2006). For example, Buick et al. (2005)
458 determined an Early Cambrian age for protoliths of metabasites and metasediments in the
459 Harts Range Metamorphic Complex (west of Alice Springs, Northern Territory, Fig. 1), based
460 on detrital zircon dating. The cores of zircons in the metabasites produced a range of ages,
461 suggesting volcaniclastic protoliths, with the youngest zircon core yielding an imprecise age
462 of 528 ± 45 Ma (Buick et al, 2001). This result suggests that further studies of Harts Range
463 are necessary in order to determine possible relationships to the Kalkarindji province.
464 Mafic intrusions of likely Cambrian age have also been reported from the
465 basement to the Canning basin in Western Australia (Fig. 1). One intrusion yielded an
466 unpublished baddelyite U-Pb SHRIMP age of ~509 Ma (D. Maidment, pers. comm.). TIMS
467 dating on baddelyite from this rock is in progress. This connection may not significantly
468 affect the size estimate of the province, if these dolerites represent feeder dykes; however, it
469 would yield insight into the deeper structures of the province.
470 Mafic intrusions in the Kanmantoo Group of the Adelaide Fold Belt (South
471 Australia, Fig. 1) yielded a TIMS U-Pb zircon age of 510 ± 2 Ma (Chen and Liu, 1996) and
472 may also be a part of the Kalkarindji LIP (Ernst and Buchan, 2003). However, this area is a
473 considerable distance (~2000 km) from the centre of the Kalkarindji Province and robust
474 geochemical and geochronological data are required to test this link. It has also been
475 speculated that mafic intrusions in the Albany-Fraser mobile belt (SW Australia, Fig. 1) form
476 part of the Kalkarindji province, based mainly on paleomagnetic studies (Harris and Li 1995).
477 If the latter relationship is proven, this would imply the existence of further extensions in

478 Antarctica, which was connected to Australia during Cambrian times. Paleomagnetism also
479 places the Tarim block of NW China, in close proximity to the Kimberley region during the
480 Early Cambrian (Li et al., 2008), which implies that counterparts of the Kalkarindji LIP could
481 also be present in China. Clearly, further studies are required to test these speculations.
482
483 6.6. Environmental impact of the Kalkarindji LIP
484 At the Early-Middle Cambrian boundary, Early Cambrian reef-builders (mainly
485 Archeocyaths) and reef-dwellers (e.g. trilobites) worldwide suffered a severe extinction of
486 more than 50% of genera (e.g. Zhuravlev and Wood, 1996; Hallam and Wignall, 1999;
487 Lasemi and Amin-Rasouli, 2007). This mass extinction has been associated with sea-level
488 fall, the so-called the Hawke Bay regression (Palmer and James, 1980), and superanoxia
489 (Hough et al, 2006). The Early-Middle Cambrian boundary is dated to 513 ± 2 Ma (Shergold
490 and Cooper, 2004). This boundary age is based on a U-Pb age, and not on $^{40}Ar/^{39}Ar$ data.
491 Uncertainties in the ^{40}K decay constants suggests that $^{40}Ar/^{39}Ar$ ages are in general 0.8 - 1.0%
492 lower than U-Pb ages in the Phanerozoic (e.g., Min et al., 2000). If correct, then the 505-508
493 Ma $^{40}Ar/^{39}Ar$ age for the Kalkarindji LIP would equate to a 509 - 513 Ma U-Pb age, thus
494 coinciding with the Early-Middle Cambrian the boundary (Glass and Phillips, 2006). The
495 possible link between the Kalkarindji LIP and the Early-Middle Cambrian mass extinction is
496 yet another example of a temporal link between LIPs and environmental events (e.g.
497 Courtillot and Renne 2003). Due to their considerable size, LIP eruptions may have induced
498 dramatic atmospheric changes, thereby affecting the climate and ocean chemistry worldwide.
499 The release of SO_2 from flood basalt eruptions has been estimated to 5 - 10 Mt for each km^3
500 of flood basalt lava (Self et al, 2005). For the eruption of the Bingy Bingy member alone (10
501 500 km^2 x 0.04km = 420 km^3), this would equate to the release of 2100 - 4200 Mt SO_2. The
502 CO_2 output would also have been immense for this eruption, on the order of 5400 Mt (13 Mt

503 CO_2 per km^3; Self et al, 2005). The outgassing of these volatiles may have played a
504 significant role in global warming, causing elevated ocean temperatures and superanoxic
505 oceans (e.g. Hough et al., 2006).
506
507 **7. Conclusions**
508 The Table Hill Volcanics, covering c. 180 000 km^2 in Western Australia and South Australia,
509 erupted at 504.6 ± 2.5 Ma (2σ). This result demonstrates that these volcanics are part of the c.
510 ~506 Ma Kalkarindji Continental Flood Basalt Province (Glass and Phillips, 2006). This
511 conclusion is supported by geochemical data from the current as well as previous studies (e.g.
512 Glass and Phillips, 2006). The two areas in question have very similar geochemical
513 characteristics with LREE enrichment coupled with low Ti, Nb and P indicating crustal
514 contamination. The chemical similarity indicates a common parentage with crustal input
515 occurring before subsequent fractionation. There are also some indications of later
516 assimilation of crustal material on a more local scale, producing subtle variations in some
517 trace element ratios.
518 By including the Table Hill Volcanics in the Kalkarindji LIP, the extent of this
519 province is estimated to $>2.1x10^6$ km^2, making it not only the oldest but also one of the
520 largest Phanerzoic LIPs. In the thickest part of the province (East Kimberley) a general
521 stratigraphy can be observed with the least fractionated rocks at the base and more
522 fractionated rocks in the upper parts of the succession. The Bingy Bingy basalt member,
523 composed mainly of glomeroporphyritic andesitic basalt in the upper part of the succession, is
524 the product of a large eruptive event, with eroded remnants covering an area of c. 10 000 km^2.
525 Research into the geochemistry, geochronology, extent and significance of the
526 Kalkarindji LIP is remains in its infancy, and a focussed dating program is required to
527 enhance our knowledge of this important LIP. The suggested coincidence with the Early-

528 Middle Cambrian mass extinction (Glass and Phillips, 2006) warrants further studies relating
529 to the architecture of this province, its size and the duration of individual eruptions.
530
531 **Acknowledgements**
532 This research was supported by a Marie Curie International Fellowship within the 6th
533 European Community Framework Programme (LZE). The Geological Survey of Western
534 Australia (GSWA) kindly allowed access and sampling approval for the Empress 1 and 1A
535 drill cores. Linda Glass (now at the Northern Territory Geological Survey) who originally
536 sampled the Empress 1 drill core, kindly provided those samples and assisted in getting the
537 sampling approval for these samples transferred to LZE. M. Stevens (GSWA) assisted in
538 sampling the Empress 1A drill core. S. Szczepanski is thanked for technical assistance with
539 acquisition of $^{40}Ar/^{39}Ar$ data in the Noble Gas Geochronology and Geochemistry Laboratory,
540 the University of Melbourne.
541
542 **References**
543 Babcock, L.E. and Peng, S., 2007. Cambrian stratigraphy: Current state and future plans.
544 Palaeogeography, Palaeoclimatology, Palaeoecology 254, 62-66.
545 Barley, M.E., Pickard, A.L., Sylvester, P.J., 1997. Emplacement of a large igneous province
546 as a possible cause of banded iron formation 2.45 billion years ago. Nature, 385,
547 55-58.
548 Bryan, S.E., Ernst, R.E., 2008. Revised definition of Large Igneous Provinces (LIPs). Earth-
549 Science Reviews 86, 175–202.
550 Buick, I.S., Hand, M., Williams, I.S., Mawby, J., Miller, J.A., Nicoll, R.S., 2005. Detrital
551 zircon provenance constraints on the evolution of the Harts Range Metamorphic

552 Complex (central Australia): links to the Centralian Superbasin. Journal of the
553 Geological Society, London. 162, 777-787.
554 Bultitude, R.J., 1976. Flood basalts of probable early Cambrian age in northern Australia. In:
555 Johnson, R.W. (Ed.), Volcanism in Australasia. New York, United States,
556 Elsevier, p. 1-20.
557 Chen, Y.D., Liu, S.F., 1996. Precise U-Pb zircon dating of a post-D2 metadolerite: constraints
558 or rapid tectonic development of the southern Adelaide Fold Belt during the
559 Cambrian. Journal of the Geological Society, London. 153, 83-90
560 Coffin, M.F. and Eldholm, O., 1994, Large Ignous Provinces: Crustal Structure, dimensions,
561 and external consequences. Reviews of Geophysics 32, 1-36
562 Compston, W., 1974, The Table Hill Volcanics of the Officer Basin—Precambrian or
563 Palaeozoic?: Geological Society of Australia Journal, v. 21, p. 403–411.
564 Courtillot, V.E., Renne, P.R., 2003. On the ages of flood basalt events. Comptes Rendus -
565 Academie des sciences. Geoscience 335, 113-140
566 Cox, K.G., Bell, J.D., Pankhurst, R.J., 1979. The Interpretation of Igneous Rocks. George
567 Allen & Unwin, London. 450 p.
568 De Min, A., Piccirillo, E.M., Marzoli, A., Bellieni, G., Renne, P.R., Ernesto, M., Marques,
569 L.S., 2003. The Central Atlantic Magmatic Province (CAMP) in Brazil;
570 petrology, geochemistry, $^{40}Ar/^{39}Ar$ ages, paleomagnetism and geodynamic
571 implications. In: Hames, W.E., McHone, J.G., Renne, P.R., Ruppel, C.R. (Eds.),
572 The Central Atlantic Magmatic Province; Insights from Fragments of Pangea.
573 Geophysical Monograph 136. American Geophysical Union, Washington, p.
574 91–128.
575 Dunn, P.R., 1963. Hodgson Downs, N.T. - 1:250 000 Geological Series. Bureau of Mineral
576 Resources, Australia Explanatory Notes SD/53-14. 16 pp

577 Eldholm, O., Coffin, M.F., 2000. Large Igneous Provinces and Plate Tectonics. In: Richards,
578 M., et al. (Eds.), The history and dynamics of global plate motions. AGU
579 Geophysical Monograph 121, 309-326.
580 Ernst, R.E., Buchan, K.L., 1997. Giant radiating dyke swarms: their use in identifying pre-
581 Mesozoic large igneous provinces and mantle plumes. In: J. Mahoney and M.
582 Coffin (Eds). Large Igneous Provinces: Continental, Oceanic, and Planetary
583 Volcanism, AGU Geophysical Monograph 100, 297-333.
584 Ernst, R. E., Buchan, K.L., 2003. Recognizing mantle plumes in the geological record.
585 Annual Review of Earth and Planetary Sciences. 31, 469-523
586 Freeman, M.J., Shergold, J.H., Morris, D.G., Walter, M.R., 1990. Late Proterozoic and
587 Paleozoic basins of Central and Northern Australia – Regional geology and
588 mineralization. In: Hughes, F.E. (Ed.), Geology of the Mineral Deposits of
589 Australia and Papua New Guinea. The Australian Institute of Mining and
590 Metallurgy, Melbourne. pp. 1125-1133.
591 Glass, L.M., 2002, Petrogenesis and Geochronology of the North Australian Kalkarinji Low-
592 Ti Continental Flood Basalt Province: PhD thesis, Canberra, Australian National
593 University.
594 Glass, L.M., Phillips, D., 2006. The Kalkarindji Continental Flood Basalt Province: A new
595 Large Igneous Province in Australia with possible links to end-Early Cambrian
596 faunal extinctions. Geology 34, 461–464.
597 Glass, L.M., Bennet.V.C., Phillips, D., 2006. Petrogenesis and geochronology of the
598 Cambrian Kalkarindji low-Ti CFB Province - northern Australia. Goldschmidt
599 Conference Abstracts 2006. Geochimica et Cosmochimica Acta 70, Supplement
600 1, A204. doi:10.1016/j.gca.2006.06.412

Gole, M., 2001. Table Hill Volcanics. Geochemistry of mafic rocks from petroleum wells Akubra 1, Boondawari 1, Yowalga 2 and Empress 1A and a surface sample. GSWA sampling approval No. S311557. Unpublished report, Ausquest Ltd. 14 p.

Gole, M., Thornett, J., 2003. Geochemistry of rocks from petroleum wells Akubra 1, Boondawari 1 and Mundadjini 1. GSWA sampling approval No. S31557. Unpublished report, Ausquest Ltd. 24 p.

Grey, K., Hocking, R.M., Stevens, M.K., Bagas, L., Carlsen, G.M., Irimies, F., Pirajno, F., Haines, P.W., Apak, S.N., 2005. Lithostratigraphic nomenclature of the Officer Basin and correlative parts of the Paterson Orogen. Western Australia Geological Survey of Western Australia, Report 93. 95 p.

Hallam, A., Wignall, P.B., 1999. Mass extinctions and sea-level changes: Earth-Science Reviews 48, 217-250.

Hanley, L.M., Wingate, M.T.D., 2000. SHRIMP zircon age for an Early Cambrian dolerite dyke: an intrusive phase of the Antrim Plateau Volcanics of northern Australia: Australian Journal of Earth Sciences 47, 1029-1040.

Harris, L.B., Li, Z.-X., 1995. Palaeomagnetic dating and tectonic significance of dolerite intrusions in the Albany Mobile, Western Australia. Earth and Planetary Science Letters 131, 143–164. doi: 10.1016/0012-821X(95)00013-3.

Hough, M.L., Shields, G.A., Evins, L.Z, Strauss, H., Henderson, R.A., Mackenzie, S., 2006. A major sulphur isotope event at c. 510 Ma: a possible anoxia-extinction-volcanism connection during the Early-Middle Cambrian transition? Terra Nova 18, 257-263.

Jackson, M.J., van de Graaf, W.J.E., 1981. Geology of the Officer Basin, Western Australia. Bureau of Mineral Resources, Australia. Bulletin 206. 102p.

626 Jourdan, F., Féraud, G., Bertrand, H., Kampunzu, A.B., Tshoso, G. Watkeys, M.K., Le Gall,
627 B., 2005. The Karoo Large Igneous Province: brevity, origin and relation with
628 mass extinction in question from new $^{40}Ar/^{39}Ar$ age data, Geology 33, 745-748.
629 Jourdan, F., Renne, P.R., 2007. Age calibration of the Fish Canyon sanidine $^{40}Ar/^{39}Ar$ dating
630 standard using primary K-Ar standards. Geochimica et Cosmochimica Acta 71,
631 387-402.
632 Jourdan, F., Féraud, G., Bertrand, H., Watkeys, M.K., Renne, P.R., 2008. $^{40}Ar/^{39}Ar$ ages of
633 the sill complex of the Karoo large igneous province: implications for the
634 Pliensbachian-Toarcian climate change. Geochemistry, Geophysics, Geosystems
635 (G3) 9, Q06009. doi:10.1029/2008GC001994
636 Jourdan, F., Marzoli, A., Bertrand, H., Cirilli, S., Tanner, L., Kontak, D., McHone, G., Renne,
637 P.R., Bellieni, G. *(Submitted to Lithos, Accepted)* $^{40}Ar/^{39}Ar$ ages of CAMP in
638 North America: implications for the Triassic-Jurassic boundary and the ^{40}K
639 decay constant bias.
640 Lasemi, Y., Amin-Rasouli, H., 2007. Archaeocyathan buildups within an entirely siliciclastic
641 succession: New discovery in the Toyonian Lalun Formation of northern Iran,
642 the Proto-Paleotethys passive margin of northern Gondwana. Sedimentary
643 Geology 201, 302–320.
644 Li, Z.X., Bogdanova, S.V., Collins A.S., Davidson, A., De Waele, B., Ernst R.E., Fitzsimons
645 I.C.W., Fuck R.A., Gladkochub D.P., Jacobs J., Karlstrom K.E., Lu, S., Natapov
646 L.M., Pease V., Pisarevsky S.A., Thrane K., Vernikovsky, V., 2008. Assembly,
647 configuration, and break-up history of Rodinia: A synthesis. Precambrian
648 Research 160, 179-210.

649 Macdonald, F. A., Wingate, M. T. D., Mitchell, K., 2005. Geology and age of the Glikson
650 impact structure, Western Australia. Australian Journal of Earth Sciences 52,
651 641-651.
652 Melluso, L., Barbieri, M., Beccaluva, L., 2004. Chemical evolution, petrogenesis, and
653 regional chemical correlations of the flood basalt sequence in the central Deccan
654 Traps, India. Proceedings of the Indian Acadademy of Science (Earth and
655 Planetary Science) 113, 587–603.
656 Min, K., Mundil, R., Renne, P.R., Ludwig, K.R., 2000. A test for systematic errors in
657 40Ar/39Ar geochronology through comparison with U–Pb analysis of a 1.1 Ga
658 rhyolite. Geochimica Cosmochimica Acta 64, 73–98.
659 Mory A. J., Beere G. M., 1988. Geology of the onshore Bonaparte and Ord basins in Western
660 Australia. Geological Survey of Western Australia, Bulletin 134.
661 Nomade, S, Knight, K.B., Beutel, E., Renne, P.R., Vérati, C., Féraud, G., Marzoli, A., Youbi
662 N., Bertrand, H., 2007. Chronology of the Central Atlantic Magmatic Province:
663 Implications for the Central Atlantic rifting processes and the Triassic–Jurassic
664 biotic crisis. Palaeogeography, Palaeoclimatology, Palaeoecology 246, 326-344.
665 Palmer, A.R., James, N.P., 1980. The Hawke Bay event: a circum Iapetus regression near the
666 Lower-Middle Cambrian boundary. In: Wones, D.R. (Ed.), Virginia Polytechnic
667 Institute and State University Memoir 2, 15–18.
668 Peers, R., 1969. A comparison of some volcanic rocks of uncertain age in the Warburton
669 Range area: Western Australia Geological Survey, Annual Report 1968, p. 57–
670 61.
671 Phillips, G., Wilson, C.J.L., Phillips, D., Szczepanski, S., 2007. Thermochronological
672 ($^{40}Ar/^{39}Ar$) evidence for Early Palaeozoic basin inversion within the southern

673 Prince Charles Mountains, East Antarctica: Implications for East Gondwana.
674 Journal of the Geological Society 164, 771-784.
675 Reddicliffe, T., 1980. Final report on exploration completed within temporary reserves 7386H
676 Rosewood, 7387H Camel Back Hills, 7388H Mud Spring Creek, 7389H Bell
677 Creek, 7390H Soda Spring, Cambridge Gulf, Western Australia. C.R.A.
678 Exploration Pty. Ltd, WAMEX Item #1196/A9527, 11 p.
679 Renne, P.R., Swisher, C.C., Deino, A.L., Karner, D.B., Owens, T.L., DePaolo, D.J., 1998.
680 Intercalibration of standards, absolute ages and uncertainties in $^{40}Ar/^{39}Ar$ dating.
681 Chemical Geology 145, 117-152.
682 Robinson, J.A.C., Wood, B.J., 1998. The depth of the spinel to garnet transition at the
683 peridotite solidus. Earth and Planetary Science Letters 164, 277-284.
684 Self, S., Thordarson, T., Widdowson, M., 2005. Gas Fluxes from Flood Basalt Eruptions.
685 Elements 5 (1), 283-287.
686 Shergold, J.H., Cooper, R.A., 2004. The Cambrian Period. In: Gradstein, F.M., et al. (Eds.), A
687 geologic time scale 2004: Cambridge, Cambridge University Press, p. 147–164.
688 Stern, R.A., Fletcher, I.R., Birger Rasmussen, B., McNaughton, N.J., and Brendan J. Griffin,
689 B.G., 2005. Ion microprobe (NanoSIMS 50) Pb-isotope geochronology at <5 m
690 scale. International Journal of Mass Spectrometry 244, 125–134.
691 Stevens, M. K., Apak, S. N. (compilers), 1999. GSWA Empress 1 and 1A well completion
692 report, Yowalga Sub-basin, Officer Basin, Western Australia: Western Australia
693 Geological Survey, Record 1999/4, 110 p.
694 Sun, S.-S., McDonough, W.F., 1989. Chemical and isotopic systematics of oceanic basalts:
695 implications for mantle composition and processes. In: Saunders, A.D., Norry,
696 M.J. (Eds.), Magmatism in the Ocean Basins. Geological Society Special
697 Publication 42, 313–345.

Sweet, I.P., Mendum, J.R., Bultitude, R.J., Morgan, C.M., 1974. The Geology of the Southern Victoria River Region, Northern Territory. Bureau of Mineral Resources, Geology and Geophysics, Report 167. Canberra, A.C.T. Australian Geological Survey Organisation. 143 p.

Townson, W.G., 1985, The subsurface geology of the western Officer Basin — results of Shell's 1980–1984 petroleum exploration campaign. APEA Journal 25, p. 34–51.

Veevers, J.J., 2004. Gondwanaland from 650–500 Ma assembly through 320 Ma merger in Pangea to 185–100 Ma breakup: supercontinental tectonics via stratigraphy and radiometric dating. Earth Science Reviews 68, 1-132.

Walter, M.R., Veevers, J.J., Calver, C.R., Grey, K., 1995. Neoproterozoic stratigraphy of the Centralian Superbasin, Australia. Precambrian Research 73, 173–195.

Zhuravlev, A.Y., Wood, R.A., 1996. Anoxia as the cause of the mid-Early Cambrian (Botomian) extinction event: Geology 24, 311-314.

713 **Figure captions**

714

715 **Figure 1**. Known extent of the Kalkarindji LIP. Cited ages (2σ errors) in the northern part
716 of the province are from Glass and Phillips (2006) and Hanley and Wingate (2000); in the
717 Savory basin from Macdonald et al (2005); and in the Officer basin from this contribution.
718 Question marks signify possible eroded remnants to the Kalkarindji province as suggested
719 previously (Ernst & Buchan, 2003; Buick et al, 2005; Glass and Phillips, 2006; Maidment,
720 pers. comm.)

721

722 **Figure 2** Selected major element oxides vs. MgO (wt%) from this study plotted with
723 previously published data (Bultitude, 1976; Hanley and Wingate, 2000; Glass and
724 Phillips, 2006).

725

726 **Figure 3**. Trace elements, normalised to primitive mantle (Sun & McDonough, 1989),
727 plotted on a spider diagram and compared with previously published data (TH003 &
728 HS002; Glass and Phillips, 2006). The distinctive pattern from altered sample 086A,
729 indicates mobility of Cs, Rb, Ba, K, Pb and Sr during alteration.

730

731 **Figure 4.** REE element values, normalised to chondrite (Boynton, 1984) compared with
732 data from Glass & Phillips (2006; TH003 & HS002).

733

734 **Figure 5.** Selected trace elements (ppm) and ratios plotted against TiO_2 (wt%) compared
735 with data from Glass & Phillips (2006; TH003 & HS002). Cr and Ni are clearly elevated
736 in the Early Antrim Plateau Volcanics, but Cu does not follow the same pattern; the Table
737 Hill Volcanics plot in two groups, one possibly representing an undepleted (in Ni and Cu)
738 Table Hill magma, as postulated by Gole and Thornett (2003). P clearly correlates with

739 Ti, but Y and Zr appear to be elevated in the Table Hill samples compared to Antrim
740 samples. This elevation is seen also in LREE and, to a lesser degree, in HREE.
741
742 **Figure 6**. Ar-Ar age and Ca/K spectra of five samples from the Table Hill Volcanics.
743 Numbers in parentheses indicate analyses performed at two different laboratories. (1) The
744 University of Melbourne; (2) The Western Australian Argon Isotope Facility. Steps
745 included in plateau age segments are shown as dark grey in colour.
746
747 **Figure 7.** Trace element ratios normalised to primitive mantle (Sun & McDonough, 1989)
748 compared with data from Glass & Phillips (2006; TH003 & HS002) and Melluso et al.
749 (2004; Deccan Traps). The Antrim and Table Hill samples cluster together due to their
750 geochemical similarity; however, there are also some differences between the Table Hill
751 and Antrim samples, possibly due to variable mixing between the magma source and a
752 crustal contaminant.

753 **Table 1**. Samples analysed in this study. * Empress 1 & 1A : GSWA samling approval S31795

Sample	Latitude	Longitude	Depth	Flow	Description
Early Antrim					
084	16°55'04"S	128°54'19"	n/a	n/a	Brown, finegrained basalt with mm-sized plagioclase phenocrysts
085	16°55'07"S	128°54'22"	n/a	n/a	Finegrained, slightly vesicular and amygdular basalt
086A	16°55'08"S	128°54'24"	n/a	n/a	Altered, intensely green, heavy rock
087	16°55'10"S	128°54'26"	n/a	n/a	Weakly porphyritic basalt, some red spotty alteration
091	16°55'16"S	128°54'22"	n/a	n/a	Mediumgrained reddish brown basalt with vague green alteration spots
022	17°30'13"S	128°17'17"	n/a	n/a	Finegrained basalt with rare vesicles, weak flow banding and small carbonate xenoliths
Main-Late Antrim					
097	16°53'59"S	128°53'58"	n/a	n/a	Finegrained red-brown basalt with feldspar laths and green-blue streaks
020	17°30'19"S	128°17'30"	n/a	n/a	Finegrained basalt with visible magnetite grains and rare vesicles
S2-33	17°21'40"S	128°19'28"	n/a	n/a	Very finegrained basalt with visible magnetite grains and rare vesicles
027	18°08'03"S	128°41'47"	n/a	n/a	Finegrained basalt with clear matrix plagioclase showing weak trachytic texture.
D04	17°22'58"S	128°19'37"	n/a	n/a	Red-brown glomeroporphyritic basalt
039	17°33'04"S	129°29'53"	n/a	n/a	Dark brown glomeroporphyritic basalt with columnar jointing.
Table Hill Volcanicsl*					
EMP1 212	27°03'13"S	125°09'24"E	212.78-212.85	6	Finegrained, slightly vesicular and weakly altered basalt. Fresh matrix feldspar 50-150 µm
EMP1A 214	"	"	214.36-214.54	6	High density, medium grained, dark grey-brown basalt. Clear feldspar, c. 200 µm
EMP1A 238	"	"	238.35-238.65	5	High density, mediumgrained, dark grey-reddish brown basalt. Clear feldspar, 100-300 µm.
EMP1 253	"	"	253.13-253.23	4	Finegrained weakly vesicular pinkish basalt. Inclusion-rich, fresh matrix feldspar 50-300 µm.
EMP1 255	"	"	255.47 – 255.56	4	Finegrained, weakly porphyritic black-brown basalt. Fresh matrix feldspar 40-350 µm
EMP1A 263	"	"	263.8-264.05	3	Grey, vesicular and amygdular basalt with slightly spotty appearance.Clear feldspar, 200-300µm
EMP1A 272	"	"	272.69-273.0	2	Finegrained brown basalt with amygdules up to 5mm. Feldspar appear slightly altered, 150 µm.

754

755 **Table 2**. Summary of Ar-Ar results. Ages are in Ma. *Curtin University, ^University of Melbourne

	$^{40}Ar/^{36}Ar$	2σ	Total-gas age	2σ	Isochron age	2σ	MSWD	Plateau age	2σ	MSWD
Whole rocks										
EMP1A 238^	339	39	487	5	480	17	70	n.a		
EMP1A 214^	614	117	540	10	465	48	35	n.a		
Plagioclase										
EMP1A 238*	160	234	486	7	521	19	58	n.a		
EMP1255*	208	166	503	2	504	7	1.7	504.6	2.5	1.6
EMP1255^	287	49	517	7	521	15	40	n.a		
EMP1253^	370	151	587	12	562	57	243	n.a		
EMP212^	368	93	522	11	487	33	83	n.a		

756

757 **Table 3**. Incompatible element ratios normalised to primitive mantle (McDonough & Sun, 1989).*Deccan values
758 from Melluso et al. (2004).

Group	Ce/Yb N	± (1 SD)	Ce/U N	± (1SD)	P/Nd N	± (1SD)	Ti/Y N	± (1SD)
Deccan*	4.0	0.8	0.7	0.2	0.7	0.1	1.3	0.3
Antrim	3.5	0.6	0.5	0.1	0.4	0.0	0.9	0.0
Table Hill	3.4	0.5	0.3	0.0	0.3	0.0	0.7	0.1

759

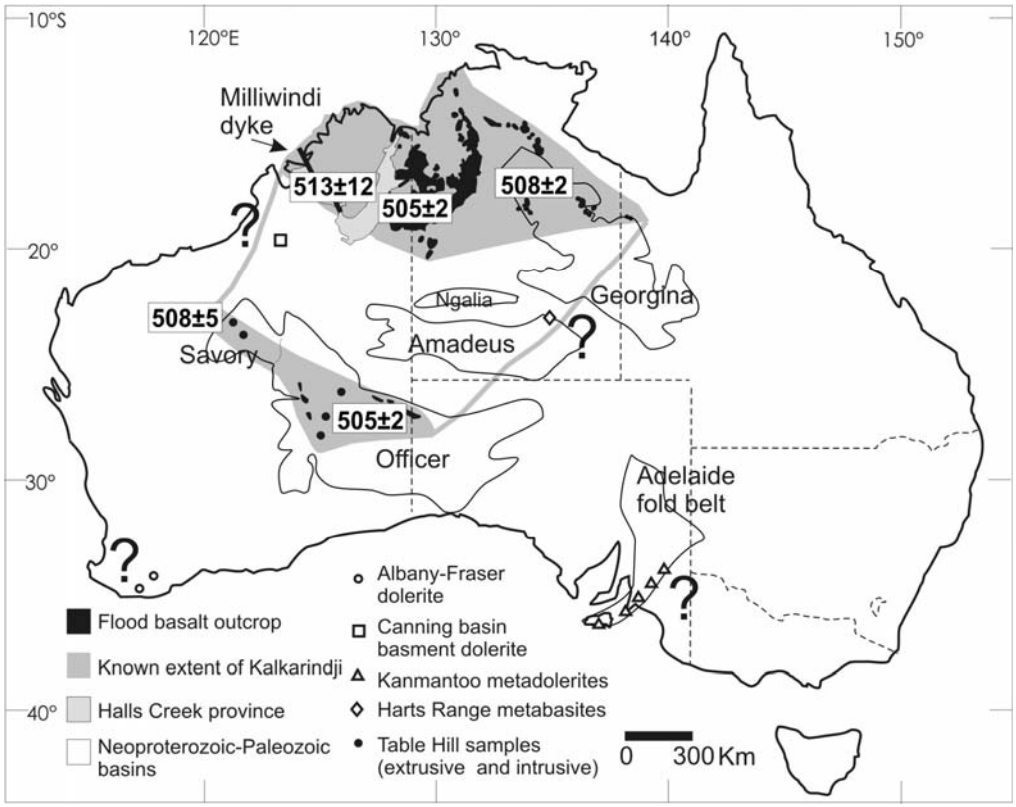

FIGURE 1

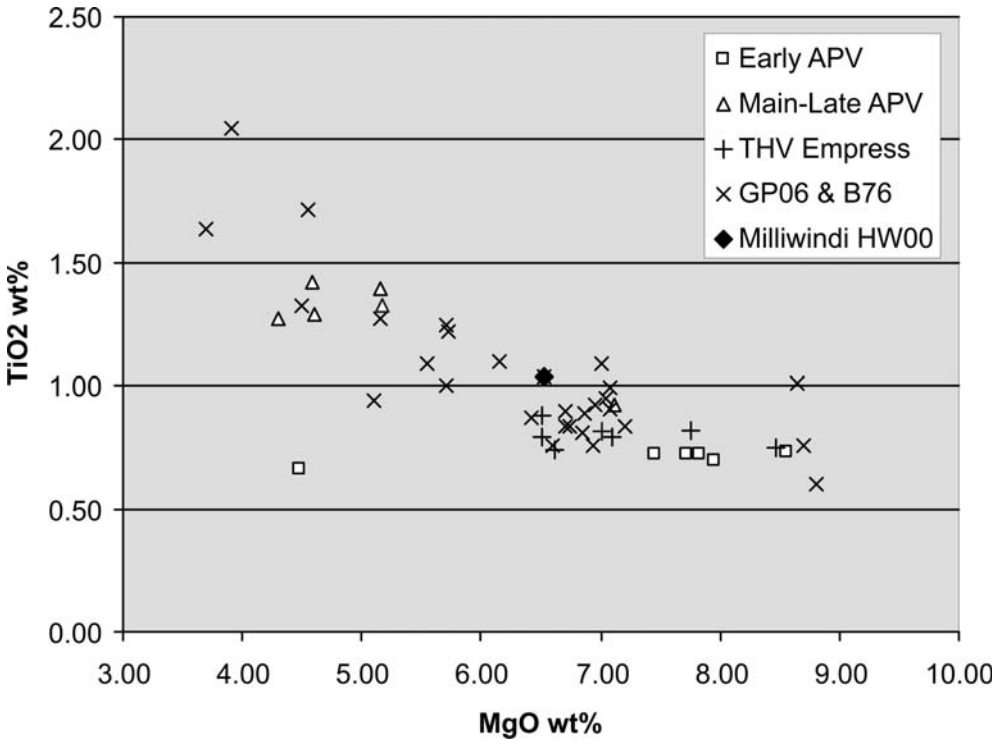

FIGURE 2

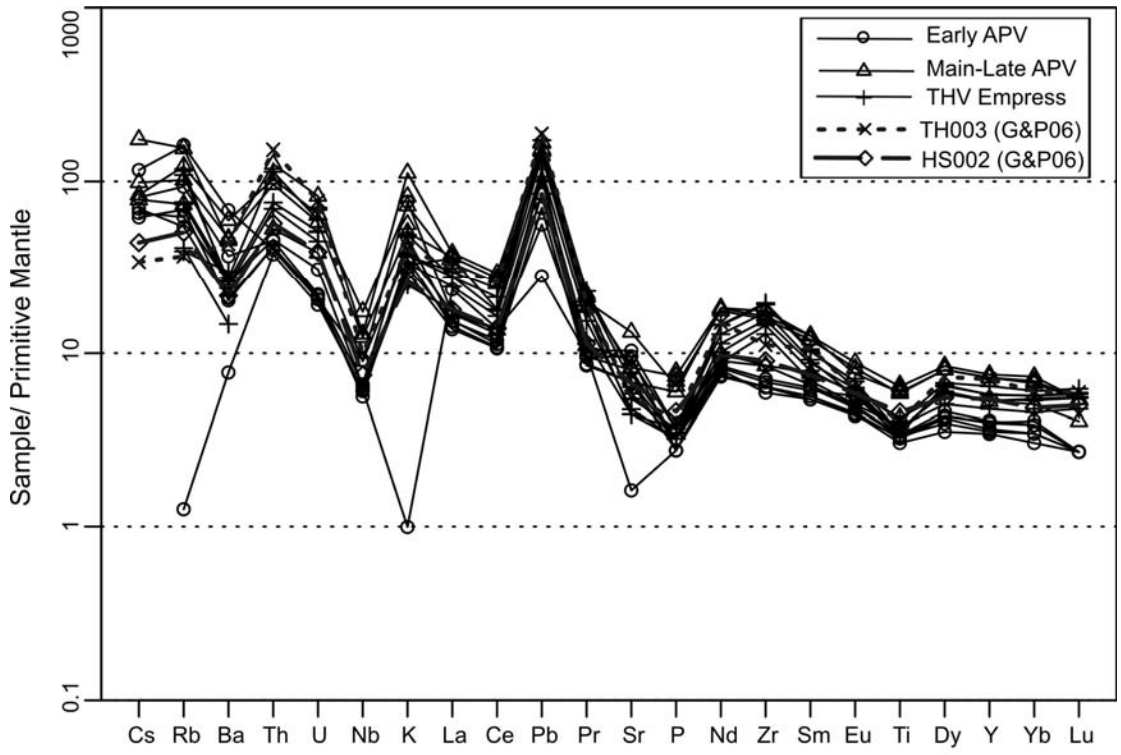
Early APV
Main-Late APV
THV Empress
TH003 (G&P06)
HS002 (G&P06)
Sample/ Primitive Mantle
1000
100
10
1
0.1
Cs Rb Ba Th U Nb K La Ce Pb Pr Sr P Nd Zr Sm Eu Ti Dy Y Yb Lu

FIGURE 3

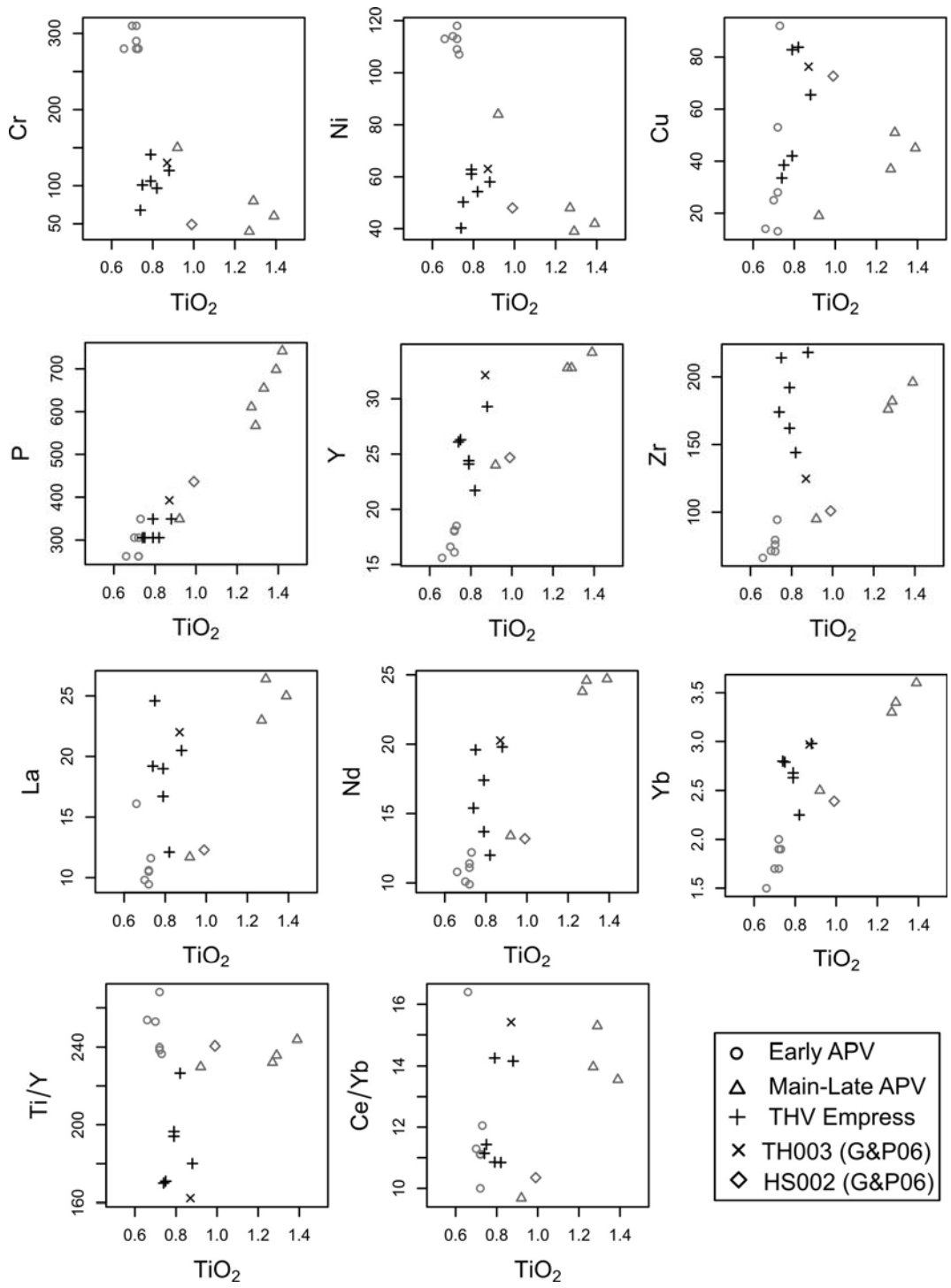
Cr
Ni
Cu
P
Y
Zr
La
Nd
Yb
Ti/Y
Ce/Yb
TiO2
Early APV
Main-Late APV
THV Empress
TH003 (G&P06)
HS002 (G&P06)

FIGURE 4.

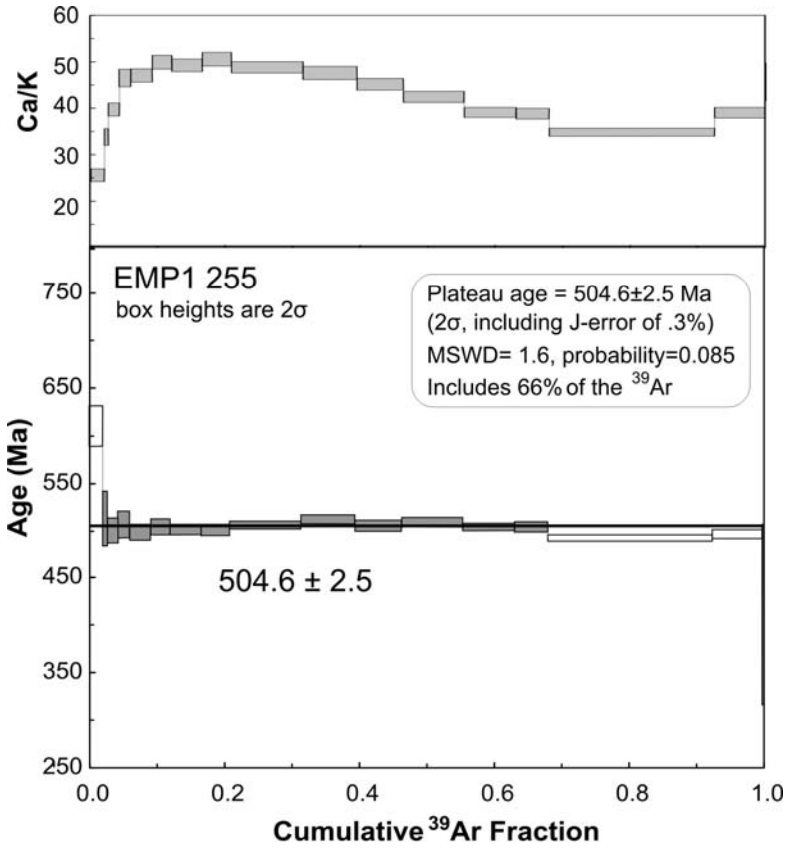

FIGURE 5

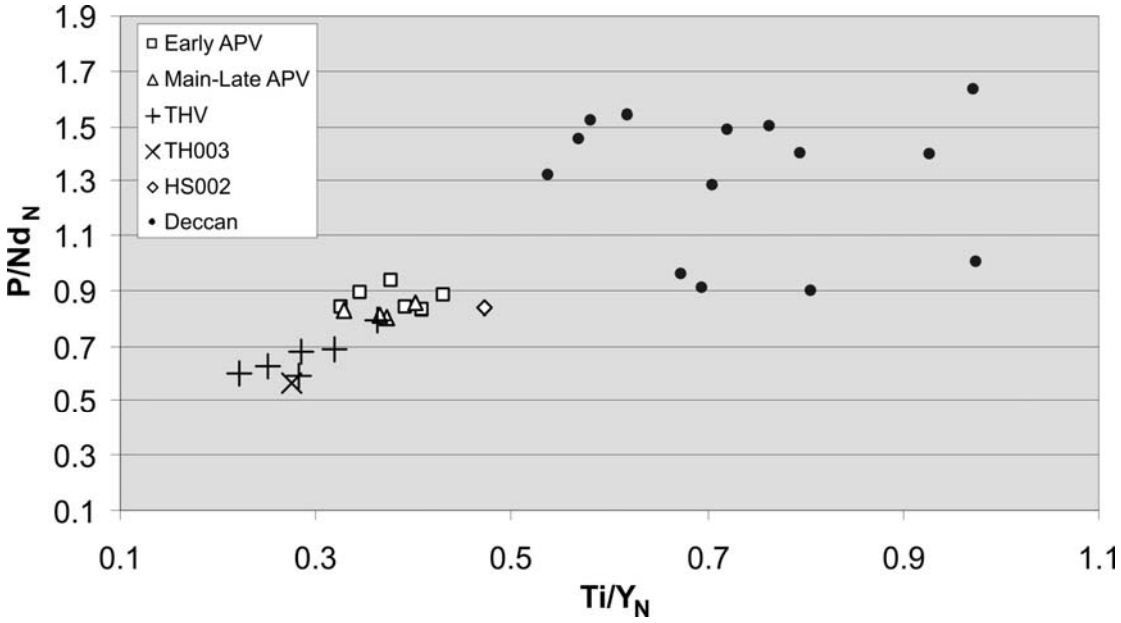

FIGURE 6

Table 1. Samples analysed in this study. * Empress 1 & 1A : GSWA samling approval S31795

Sample	Latitude	Longitude	Depth	Flow	Description
Early APV					
084	16°55'04"S	128°54'19"	n/a	n/a	Brown, finegrained basalt with mm-sized plagioclase phenocrysts
085	16°55'07"S	128°54'22"	n/a	n/a	Finegrained, slightly vesicular and amygdular basalt
086A	16°55'08"S	128°54'24"	n/a	n/a	Altered, intensely green, heavy rock
087	16°55'10"S	128°54'26"	n/a	n/a	Weakly porphyritic basalt, some red spotty alteration
091	16°55'16"S	128°54'22"	n/a	n/a	Mediumgrained reddish brown basalt with vague green alteration spots
022	17°30'13"S	128°17'17"	n/a	n/a	Finegrained basalt with rare vesicles, weak flow banding and small carbonate xenoliths
Main-Late APV					
097	16°53'59"S	128°53'58"	n/a	n/a	Finegrained red-brown basalt with feldspar laths and green-blue streaks
020	17°30'19"S	128°17'30"	n/a	n/a	Finegrained basalt with visible magnetite grains and rare vesicles
S2-33	17°21'40"S	128°19'28"	n/a	n/a	Very finegrained basalt with visible magnetite grains and rare vesicles
027	18°08'03"S	128°41'47"	n/a	n/a	Finegrained basalt with clear matrix plagioclase showing weak trachytic texture.
D04	17°22'58"S	128°19'37"	n/a	n/a	Red-brown glomeroporphyritic basalt
039	17°33'04"S	129°29'53"	n/a	n/a	Dark brown glomeroporphyritic basalt with columnar jointing.
*THV**					
EMP1 212	27°03'13"S	125°09'24"E	212.78-212.85	6	Finegrained, slightly vesicular and weakly altered basalt. Fresh matrix feldspar 50-150 µm
EMP1A 214	"	"	214.36-214.54	6	High density, medium grained, dark grey-brown basalt. Clear feldspar, c. 200 µm
EMP1A 238	"	"	238.35-238.65	5	High density, mediumgrained, dark grey-reddish brown basalt. Clear feldspar, 100-300 µm.
EMP1 253	"	"	253.13-253.23	4	Finegrained weakly vesicular pinkish basalt. Inclusion-rich, fresh matrix feldspar 50-300 µm.
EMP1 255	"	"	255.47 – 255.56	4	Finegrained, weakly porphyritic black-brown basalt. Fresh matrix feldspar 40-350 µm
EMP1A 263	"	"	263.8-264.05	3	Grey, vesicular and amygdular basalt with slightly spotty appearance.Clear feldspar, 200-300µm
EMP1A 272	"	"	272.69-273.0	2	Finegrained brown basalt with amygdules up to 5mm. Feldspar appear slightly altered, 150 µm.

Table 2. APV Chemistry data. Majors by XRF (AAC, JCU) and trace elements by ICP-MS (SGS, Perth).

Sample	084	085	086A	087	091	022	097	020	S2-33	027	D04	039
Major elements (wt%)												
SiO2	51.4	51.4	41.6	50.8	51.1	51.2	53.6	51.5	53.2	53.8	51.5	53.5
TiO2	0.72	0.72	0.66	0.72	0.70	0.73	1.42	0.92	1.33	1.39	1.27	1.29
Al2O3	16.1	16.1	17.4	15.9	16.1	15.6	13.5	15.1	14.1	14.6	16.0	14.5
Fe2O3t	8.65	8.33	8.24	8.33	8.77	8.65	12.3	10.5	11.8	11.5	11.2	11.7
MnO	0.13	0.14	0.16	0.13	0.13	0.14	0.13	0.18	0.19	0.17	0.15	0.18
MgO	7.82	7.45	4.47	7.72	7.96	8.55	4.59	7.11	5.17	5.15	4.30	4.60
CaO	10.9	9.29	21.1	11.2	10.7	8.62	5.57	9.26	6.99	8.53	7.39	6.77
Na2O	1.86	2.88	0.00	1.58	1.52	2.10	2.61	2.72	3.31	2.08	3.04	2.28
K2O	0.96	1.42	0.03	0.89	1.07	2.30	2.46	1.18	1.70	1.53	2.18	3.37
P2O5	0.07	0.06	0.06	0.06	0.07	0.08	0.17	0.08	0.15	0.16	0.14	0.13
Total	99.9	100.2	99.4	99.7	99.9	100.2	99.3	99.6	99.8	100.3	99.6	99.9
Trace elements (ppm)												
Ti	4440	4610	3860	4120	4050	4780		6090		>10000	>10000	>10000
S	60	30	410	30	20	260		30		720	90	30
Sc	37	38	30	36	35	41		45		39	39	41
V	189	202	181	185	195	207		275		278	269	302
Cr	280	310	280	290	310	280		150		60	40	80
Ni	113	118	113	109	114	107		84		42	48	39
Co	76.2	55.2	53.1	59.3	54.5	76.8		83.9		62.5	67.9	82.1
Cu	13	53	14	28	25	92		19		45	37	51
Ga	16.5	16.3	29.3	15.5	15.9	16.9		19.3		20.5	22.4	20.9
Rb	39.5	59.2	0.8	34.7	43.6	102		46.9		64.7	77.7	98.3
Sr	168	202	34.2	143	144	218		191		174	279	143
Y	18.1	18	15.6	16.1	16.6	18.5		24		34.2	32.8	32.8
Zr	76	79.4	66.2	71	71.4	94.4		94.9		196	176	182
Nb	4.6	4.7	4.4	4.3	4	6.5		6.4		8.8	12.4	9.2
Sn	1	0.8	0.7	0.8	0.7	0.8		1.3		1.8	1.6	2
Cs	0.52	0.64		0.55	0.49	0.92		0.62		0.78	0.66	1.37
Ba	181	258	54	146	141	477		177		328	417	319
La	10.6	10.5	16.1	9.44	9.81	11.6		11.7		25	23	26.4
Ce	20	21.1	24.6	18.9	19.2	22.9		24.2		48.8	46.1	52
Pr	2.64	2.61	2.72	2.34	2.38	2.85		3.05		5.83	5.51	6.08
Nd	11.1	11.4	10.8	9.9	10.1	12.2		13.4		24.7	23.8	24.6
Sm	2.7	2.8	2.4	2.4	2.5	2.9		3.4		5.6	5.3	5.6
Eu	0.95	0.81	0.75	0.73	0.76	0.83		1		1.48	1.37	1.27
Gd	3.3	3.3	2.7	2.8	3	3.3		4.1		6.2	5.9	5.9
Tb	0.54	0.47	0.38	0.4	0.43	0.47		0.59		0.91	0.84	0.84
Dy	3.2	3.2	2.6	2.9	3.1	3.4		4.3		6.2	5.9	5.9
Ho	0.71	0.64	0.53	0.56	0.6	0.66		0.86		1.22	1.16	1.13

Tm	0.31	0.28	0.23	0.24	0.26	0.28		0.38		0.54	0.51	0.5
Yb	2	1.9	1.5	1.7	1.7	1.9		2.5		3.6	3.3	3.4
Lu	0.2	0.2	0.2	0.2	0.2	0.2		0.3		0.4	0.4	0.4
Hf	1.8	1.8	1.5	1.6	1.7	2		2.2		4.3	3.9	4
Ta	1.4	1.2	1.1	1.2	1.1	1.5		1.6		1.7	2.1	2
Pb	8	6	2	5	5	4		6		10	11	12
Th	3.92	3.86	3.21	3.56	3.55	3.42		4.52		8.18	8.79	10.7
U	0.65	0.46	0.4	0.43	0.45	0.43		0.81		1.22	1.36	1.73

Table 3. THV Chemistry data. Majors by XRF (AAC, JCU) and trace elements by ICP-MS (AAC. JCU).

Sample	Emp1_212	Emp1_253	Emp1_255	Emp1A_214	Emp1A_238	Emp1A_263	Emp1A_272.69
SiO2	50.69	53.15	52.51	52.06	52.32	52.09	47.77
TiO2	0.82	0.79	0.88	0.79	0.74	0.8	0.75
Al2O3	15.29	15.6	15.23	15.27	15.11	15.26	16.49
Fe2O3t	10.16	9.03	9.5	10.22	10.02	9.2	8.44
MnO	0.13	0.14	0.13	0.15	0.21	0.08	0.04
MgO	7.75	6.51	6.5	7.1	6.62	7.01	8.46
CaO	9.79	8.75	8.55	9.55	9.16	7.27	6.5
Na2O	1.8	1.79	1.92	2	2.48	2.08	2.16
K2O	0.75	1.48	1.12	1.01	1.12	1.03	0.99
P2O5	0.07	0.08	0.08	0.07	0.07	0.08	0.07
Total	100.91	99.72	100.26	100.92	100.79	100.85	100.79
Ti	4850	4720	5370	8260	7900		8330
Sc	36.1	29.5	32.5	35.3	36.2		34
V	246	191	216	154	213		178
Cr	96.7	141	120	106	67.9		101
Ni	54.3	62.8	58	61	40.3		50.3
Co	69.3	53.3	61.2	52.8	47.8		43
Cu	83.8	42	65.5	82.8	33.5		38.5
Ga	24.2	23.2	25.4	28.2	29.4		29.6
Rb	26.1	46.9	25	74.9	69.2		48.2
Sr	93.6	93.5	115	100	123		161
Y	21.7	24.4	29.3	24.1	26.1		26.3
Zr	144	192	218	162	174		214
Sn	1.79	1.84	2.45	1.06	0.78		1.5
Ba	103	181	209	174	185		193
La	12.1	19	20.5	16.7	19.2		24.6
Ce	24.4	37.5	42.2	29.1	31.2		31.9
Pr	3.27	4.9	5.53	4.24	4.77		6.32
Nd	12	17.4	19.8	13.7	15.4		19.6
Sm	3.07	4.06	4.67	3.51	3.89		4.54
Eu	0.849	0.938	1.06	0.977	1.04		1.15
Gd	3.59	4.42	5.02	4.15	4.53		4.88
Tb	0.637	0.763	0.874	0.756	0.826		0.842
Dy	3.74	4.34	4.95	4.43	4.82		4.73
Ho	0.832	0.946	1.08	0.964	1.04		0.981
Er	2.32	2.68	3.05	2.71	2.9		2.74
Tm	0.338	0.392	0.448	0.404	0.434		0.42
Yb	2.25	2.63	2.98	2.68	2.8		2.79
Lu	0.353	0.407	0.46	0.413	0.437		0.43
Pb	7.25	11.1	10.2	8.35	9.97		12.2
Th				5.91	6.42		9.67
U	1.07	1.44	1.48	0.945	1.08		1.26

Table 4. Summary of Ar-Ar results. Ages are in Ma. *Curtin University, ^University of Melbourne

	$^{40}Ar/^{36}Ar$	2σ	Total-gas age	2σ	Isochron age	2σ	MSWD	Plateau age	2σ	MSWD
Whole rocks										
EMP1A 238^	339	39	487	5	480	17	70	n.a		
EMP1A 214^	614	117	540	10	465	48	35	n.a		
Plagioclase										
EMP1A 238*	160	234	486	7	521	19	58	n.a		
EMP1255*	208	166	503	2	504	7	1.7	504.6	2.5	1.6
EMP1255^	287	49	517	7	521	15	40	n.a		
EMP1253^	370	151	587	12	562	57	243	n.a		
EMP212^	368	93	522	11	487	33	83	n.a		

Table 5. Incompatible element ratios normalised to primitive mantle (McDonough & Sun, 1989)*Deccan values from Melluso et al. (2004).

Group	Ce/Yb N	± (1 SD)	Ce/U N	± (1SD)	P/Nd N	± (1SD)	Ti/Y N	± (1SD)
Deccan*	4.0	0.8	0.7	0.2	0.7	0.1	1.3	0.3
APV	3.5	0.6	0.5	0.1	0.4	0.0	0.9	0.0
THV	3.4	0.5	0.3	0.0	0.3	0.0	0.7	0.1